International Journal of Engineering Research and Development

DOI: 10.29137/ijerad.1475281

Volume:17 Issue:01 Pages:115-125 March/2025

Research Article

Effect of Different Heat Pipe Lengths on Heat Transfer in Battery Cooling Systems

Emre Torun[1*], Ertan Buyruk[1]

[1] Cumhuriyet University, Faculty of Engineering, Department of Mechanical Engineering, 58140, Sivas

***Received**: 29/04/2024 **Accepted**: 10/10/2024 **Published Online:** 15/03/2025*
***Final Version**: 01/03/2025*

Abstract

Today, electric vehicles are widely used around the world. Although lithium-ion batteries, which are one of the most commonly used battery types in electric vehicles, have many advantages, they release large amounts of heat during operation, which causes the battery temperature to rise, resulting in performance and safety problems. To overcome these problems and keep the batteries in the optimum temperature range, heat pipe systems have been used in recent years and the effect of heat pipe systems on battery cooling performance has been investigated in many studies. In this study, battery modules formed with heat pipes of different lengths, 15 cm and 17 cm, were examined at different discharge rates of 1C, 3C and 5C to investigate the effect of heat pipe length on battery cooling performance. It was observed that the short heat pipe system reduced the maximum battery surface temperature from 23.19°C to 22.93°C at 1C discharge rate, from 29.26°C to 28.94°C at 3C discharge rate and from 34.12°C to 33.89°C at 5C discharge rate. It was calculated that the temperature difference between the evaporator and condenser sections of the heat pipe decreased from 1.04°C to 0.83°C at 1C flow rate, from 5.36°C to 4.29°C at 3C flow rate, and from 14.91°C to 11.93°C at 5C flow rate in the short heat pipe system compared to the long heat pipe system, and it was determined that the temperature difference between the evaporator and condenser sections was 20% less in the short pipe system, resulting in faster cooling.

Keywords

"Lithium-ion battery, heat pipe, battery thermal management systems, heat transfer"

**** Corresponding Author:** emretorun@gmail.com*

1. Introduction

In recent years, the demand for electric vehicles has been in a continuous upward trend. Electric vehicles receive the electrical energy they need from the battery systems they contain. Lithium-ion type batteries, which are widely used in electric vehicles, are more suitable and efficient than other battery types due to their low self-discharge rate, long battery life, high energy storage density and light weight (Etacheri et al., 2011). Despite these advantages, lithium-ion batteries have some disadvantages such as high heat generation, temperature-dependent performance and overcharging (Maleki & Howard, 2006; Belov & Yang, 2008).

Lithium-ion batteries release high levels of heat energy while charging or discharging after use due to the reactions within the battery and the internal resistance of the battery, and this heat causes the battery temperature to increase and the battery efficiency to decrease. Studies have revealed that the battery cell temperature should be kept in the range of 15°C - 40°C in order to obtain maximum efficiency from batteries (Pesaran, 2001; Jouhara et al., 2019; Ramadass et al., 2022; Url-1, 2022). In addition, the maximum temperature difference within the battery module should be below 5°C in order to obtain high efficiency from the battery module and to prolong the battery life (Pesaran, 2002; Park & Jaura, 2003; Mahamud & Park, 2011; Greco, 2015; Rao, 2017; Wu, 2019). Therefore, the battery system should be thermally managed and the batteries should not be allowed to rise above a certain temperature value.

Air, water, mineral oil, phase change materials, heat pipes, thermoelectric modules or their combinations can be used for cooling battery modules. In recent years, heat pipes, which are an artificial component, have been widely used especially in cooling systems due to their high heat transfer capability, low space requirements, no need for energy during operation, no maintenance costs and long service life (Tiari, 2016). To date, many researchers have designed hybrid battery cooling systems with heat pipes and phase change material (PCM) and investigated the cooling performance of the designed systems at different discharge rates. Karimi et al. (2021) designed a system with 6 copper heat pipes and PCM glued on a prismatic lithium-ion battery and achieved a 35% temperature reduction compared to natural convection. Zhang et al. (2020) obtained a better cooling performance compared to the natural and forced convection case with their design with composite PCM obtained from heat pipes, paraffin and metal foam. Chen et al. (2021) found that there was a temperature decrease of about 30% by adjusting the thickness of the PCM in the system they designed with heat pipes, PCM and battery. In the studies, each researcher has examined the cooling performance of the systems they have created by applying a different design with PCM and heat pipes, but it is seen that there is not enough research in the literature on the effect of heat pipe length on cooling performance, and it is thought that this study will contribute to the literature.

Within the scope of this study, unlike the existing studies, in order to examine the variation of the cooling performance of the system formed with heat pipes and PCM according to the length of the heat pipe, a different block design consisting of two different length heat pipe groups of 15 and 17 cm and 2 aluminium blocks containing PCM in contact with the condenser and evaporator parts of the heat pipe was made. The battery cells were placed in 9 battery slots in the first block, and both blocks were designed as both chambered to contain PCM and channelled to transmit the heat accumulated in the first block to the second block with heat pipes. The system was discharged at a constant ambient temperature of 20°C and at different discharge rates of 1C, 3C and 5C. The effect of the heat pipe length on the cooling performance of the system was analysed by comparing the maximum surface temperatures of the batteries and the maximum surface temperature differences of the batteries.

Symbols and Abbreviations

Q	Heat Transfer
Q_{max}	Maximum Heat Transfer
L	Length
$\boldsymbol{L_{evaporation}}$	Length of Evaporation Section
$\boldsymbol{L_{condensation}}$	Length of Condensation Section
L_{eff}	Heat Pipe Effective Length
$R_{thermal}$	Thermal Resistance
k_{eff}	Effective Heat Transfer Coefficient
A_{hp}	Cross-Sectional Area of The Heat Pipe
T	Temperature
ΔT	Temperature Difference
I	Current
V	Voltage
V_{oc}	Battery Open Circuit Voltage
V_{cut}	Cut-Off Voltage
C	Charge/discharge rate
SOC	State of Charge
PCM	Phase Change Material

2. Material and method

2.1. Battery Module

In this study, 9 cylindrical lithium-ion batteries of type 18650 were used for the battery module, and three series and three parallel connections (3S3P) battery module were formed. The type of lithium-ion battery used was nickel manganese cobalt oxide (LiNiMnCoO2). The number of battery cells forming the battery module and their connection types were selected as 9 by making 3 parallel and 3 serial connections according to the maximum current, voltage and power values of the electronic load device used in the discharge test of the battery module.
The thermal, physical and electrical properties of the battery cells used are given in Table 1 and the electrical properties of the battery module are given in Table 2.

Table 1. Thermal, Physical and Electrical Properties of The Battery

Battery Type	18650, Lithium İon
Battery Shape	Cylindrical
Battery Chemical Component	$LiNiMnCoO_2$
Nominal Capacity	2000 mAh
Nominal Voltage	3.7 V
Height	65 mm
Diameter	18 mm
Thermal Conduction Coefficient	3 W/mK
Battery Specific Heat	1000 J/kgK
Density	2539 kg/m^3
Charging Cut-Off Voltage	4.2 V
Discharge Cut-Off Voltage	3.0 V

Table 2. Electrical Characteristics of The Battery Module

Number of Batteries	9 pieces
Connection style	3 serial and 3 parallel (3S3P)
Nominal Capacity	6000 mAh
Nominal Voltage	11.1 V

2.2. Heat Pipes

Heat pipes consist of three main sections as shown in Figure 1: evaporator section, adiabatic section and condenser section.

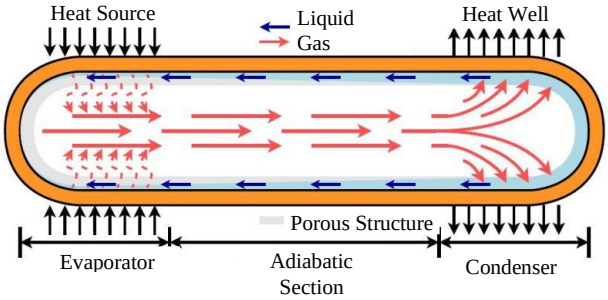

Figure 1. Heat Pipe Structure, Sections and Working System

As shown in Figure 2, heat pipes have a porous, ducted or screened structure that creates a capillary effect on the walls within the copper jacket and the internal ambient pressure is negative. Air, distilled water, etc. are used as fluid inside. In addition, heat pipes can be produced as geometrically cylindrical and flat, straight or twisted in shape according to the intended use.

As the working principle of heat pipes, when the evaporator section of the heat pipe is heated, the working fluid in the heat pipe boils at a temperature lower than the normal boiling temperature because the medium is at negative pressure and becomes vapour and the vapour formed moves to the condenser section due to the pressure difference. The vapour advancing to the condenser section becomes

liquid again by giving off the heat it has here and advances to the evaporation section again due to the capillarity effect of the porous structure on the pipe walls and the cycle continues in this way until the temperature balance is established. Studies have shown that the thermal conductivity of the heat pipe is almost 90 times higher than that of a copper rod of the same size (Faghri, 1995). In practice, the evaporator section of the heat pipe is brought into contact with the battery module, while the condenser section is brought into contact with the external environment or the cooling section.

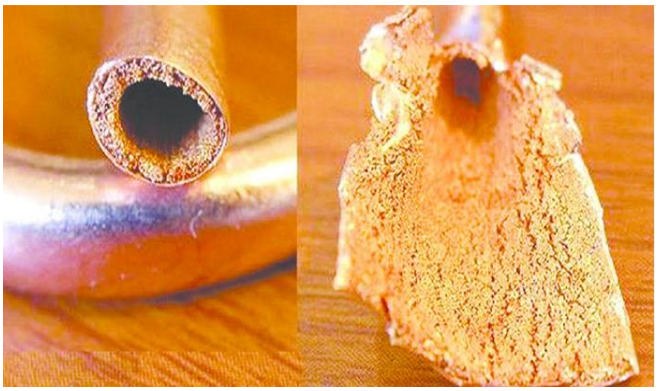

Figure 2. Porous Structure on The Inner Walls of The Heat Pipe

The heat transfer (Q) value through heat pipes can be found with the help of equation (1), the heat pipe effective length (L_{eff}) value can be found with the help of equation (2) and the thermal resistance ($R_{thermal}$) value can be found with the help of equation (3) (Ghanbarpourgeravi, 2017). In these equations, k_{eff} is the effective heat transfer coefficient of the heat pipe, A_{hp} is the cross-sectional area of the heat pipe and ΔT is the temperature difference between the evaporation and condensation sections.

$$\boldsymbol{Q = \frac{k_{eff}.A_{hp}}{L_{eff}}.\Delta T} \tag{1}$$

$$\boldsymbol{L_{eff} = L_{adiabatic} + \left(\frac{L_{evaporation}+L_{condensation}}{2}\right)} \tag{2}$$

$$R_{thermal} = \frac{L_{eff}}{k_{eff}.A_{hp}} \tag{3}$$

2.3. Cooling System Designs

In this study, two different systems were designed with 15 cm and 17 cm long heat pipes. Thus, the effect of heat pipe length on battery cooling performance could be analysed. In both systems, there are composite PCM, fin and fan in aluminium blocks. The system with 17 cm heat pipes is named as S1 and the system with 15 cm heat pipes is named as S2. The schematic representation and isometric view of the systems are given in Figure 3.a and Figure 3.b, and the visuals of the S1 and S2 systems are given in Figure 4 and Figure 5. The evaporator section of the heat pipe is placed in the first aluminium block where the coils are located and the condenser section is placed in the second aluminium block where the fin is located. In the S1 system, the length of the adiabatic part of the heat pipe is 3 cm, the length of the condensing part is 4 cm and the length of the evaporation part is 10 cm, making the total effective length of the heat pipe 10 cm, while in the S2 system, the length of the adiabatic part of the heat pipe is 1 cm, the length of the condensing part is 4 cm and the length of the evaporation part is 10 cm, making the total effective length of the heat pipe 8 cm. The cross-sectional area of the heat pipes used in both systems is equal and the effective heat transfer coefficients are also equal since the same type of heat pipes are used. The effective heat transfer coefficient of the heat pipe was selected as 9216 W/mK as in similar studies in the literature (Behi et al., 2020). The properties of the heat pipes used are given in Table 3.

Table 3. Heat Pipe Properties Used in S1 and S2 Systems

	S1 System	S2 System
L_{eff} (m)	0,1	0,08
k_{eff} (W/mK)	9216	9216
A_{hp} (m^2)	2,4e-5	2,4e-5

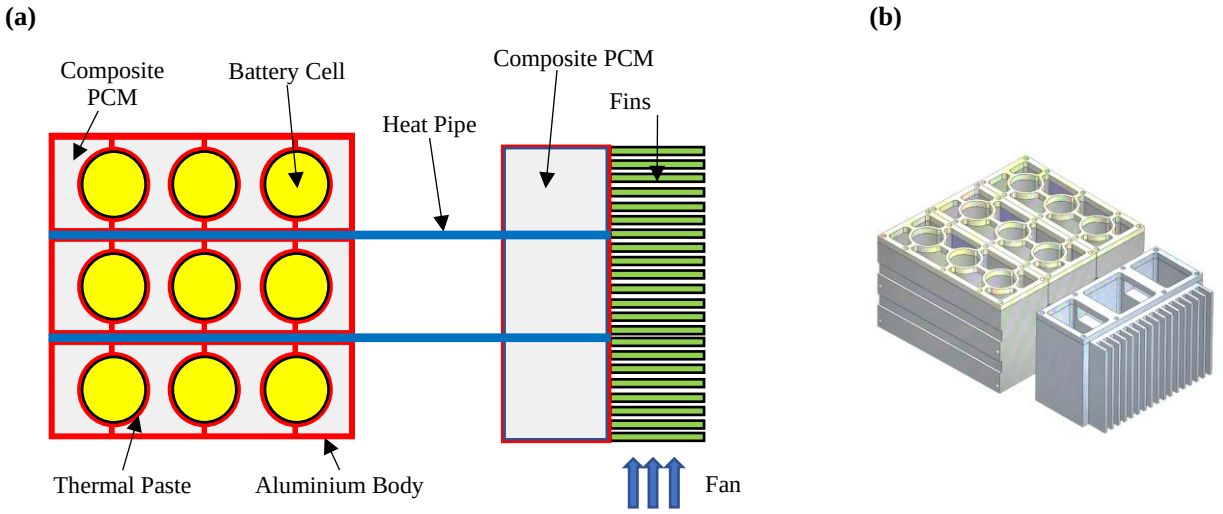

Figure 3. (a) Schematic Representation of The Designed Battery Cooling System; **(b)** Designed Battery Cooling System Isometric View

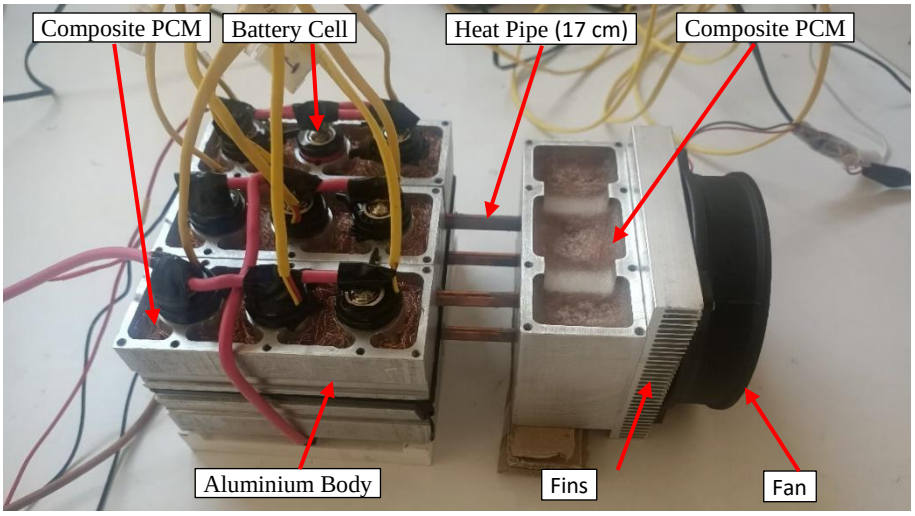

Figure 4. System with 17 cm Long Heat Pipes (S1)

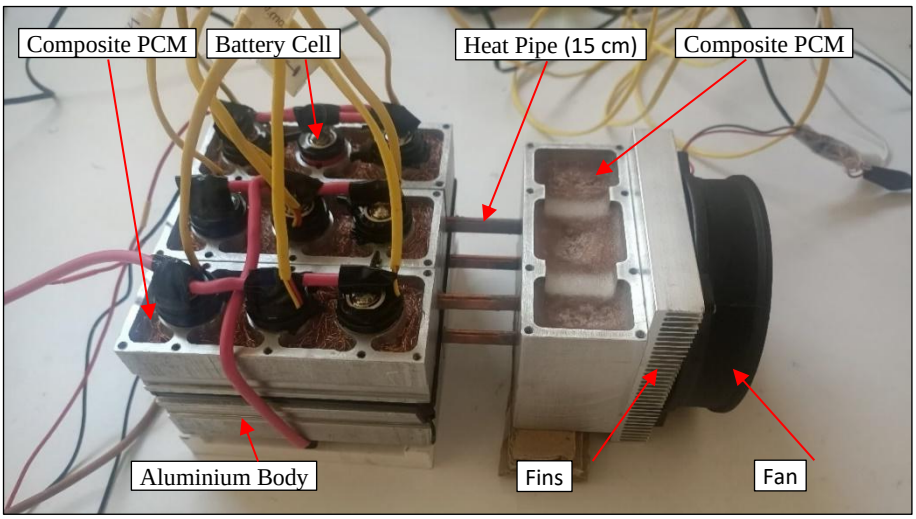

Figure 5. System with 15 cm Long Heat Pipes (S2)

2.4. Experimental Setup and Performance Tests

As the experimental setup, 9 cylindrical 18650 model cylindrical lithium ion batteries (LiNiMnCoO2) with a capacity of 2000 mAh and a voltage value of 3.7 V, 1 Electronic Load Device (40 A, 15 Volt, 400 Watt) to discharge the batteries, 10 K type thermocouples (±0, 5ºC temperature reading accuracy), 1 data logger to record the data at certain times, 1 battery charger (5 A - 12.6 V) to recharge the batteries when they are discharged and 1 computer to process the data. In this experiment, UNI-T brand and UTL8211 model electronic load device (400 watt power, ± 0.05% accuracy) was used. The data logger used is MC Measurement Computing brand and USB-2416 model and is capable of recording temperature values with an accuracy of ±0.457ºC. IMAX brand B6 model charger (6 A), which has the ability to charge each battery series in the module in a balanced way without voltage difference between them, was used as a charger for charging after the battery discharge process. The experimental setup used is shown in Figure 6.

The battery cooling systems proposed in this study were discharged at 1C, 3C and 5C discharge rates at constant ambient temperature. The general operating temperature of 20°C was selected as the ambient temperature. Therefore, a total of 6 experiments were performed for all systems, 3 different experiments for each proposed system, and the current and voltage values applied in the experiments are shown in Table 4. The temperature change in the battery cells over time was recorded with a data logger and the change of temperatures according to the battery charge rate was calculated. V_{oc} open circuit voltage expressed in Table 4 is the value read when both ends of the battery are idle, that is, when the battery is not loaded, and V_{cut} battery discharge cut-off voltage is the voltage value at which the discharge process is stopped while discharging the batteries.

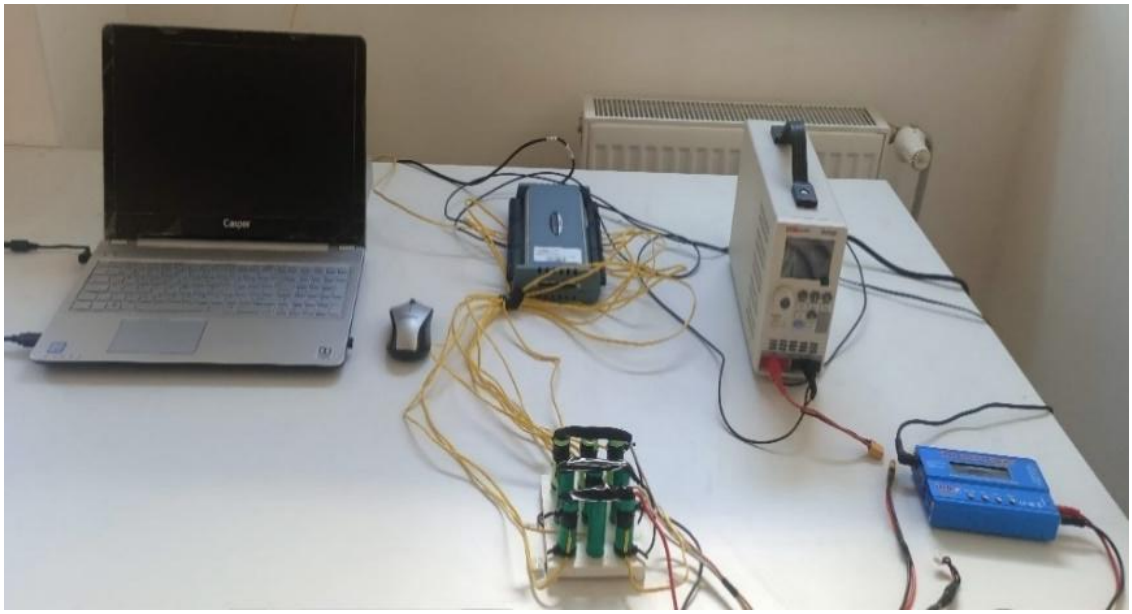

Figure 6. Experimental Setup Visualisation

Table 4. Tests and Voltage Values Applied to The Battery Module

	Test-1	Test-2	Test-3
Discharge Rate, C	1C	3C	5C
Applied Discharge Current, I	6 Ampere	18 Ampere	30 Ampere
Battery Open Circuit Voltage, V_{oc}	12,6 V	12,6 V	12,6 V
Battery Discharge Cut-Off Voltage, V_{cut}	9,0 V	9,0 V	9,0 V

3. Results and Discussion

3.1. Performance of the Systems at 1C Discharge Rate

Figure 7 and Figure 8 show the maximum surface temperatures and maximum surface temperature differences obtained at 20°C ambient temperature of the module (S1) using composite PCM, aluminium block, 17 cm heat pipes and fan and the module (S2) using composite PCM, aluminium block, 15 cm heat pipes and fan at 1C discharge rate. The difference of S2 module from S1 module is that shorter heat pipes are used.

It was observed that the designed S2 module reduced the maximum surface temperature from 23.19°C to 22.93°C by approximately 1% compared to the S1 system. It is also observed that the maximum battery surface temperature differences obtained in both systems are very close to each other and average 0.45°C. Therefore, at a discharge rate of 1C, the S2 system exhibited a better cooling

performance than the S1 system. In both cases, the maximum surface temperatures are below the permissible operating temperature of 40°C and the maximum surface temperature differences are below the permissible 5°C.

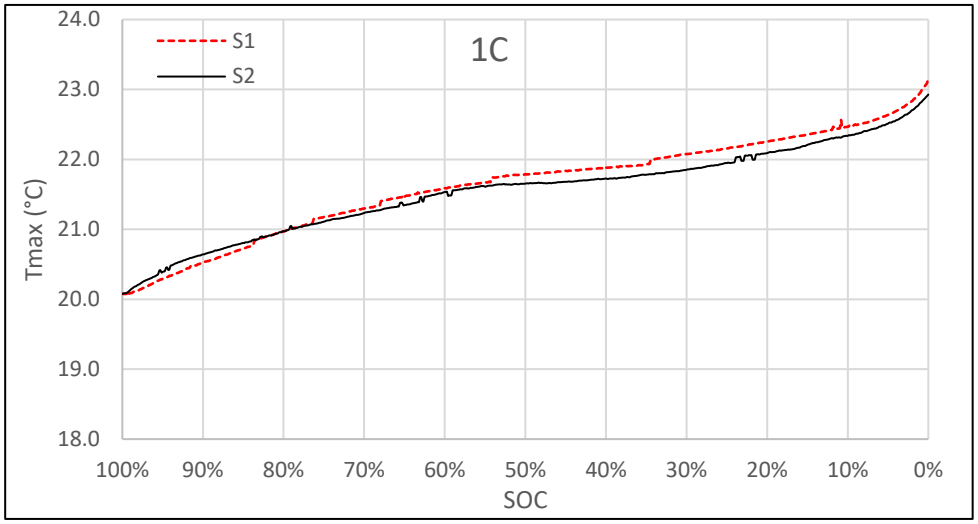

Figure 7. Maximum Surface Temperatures of S1 and S2 Systems at 20°C Ambient Temperature at 1C Discharge Rate

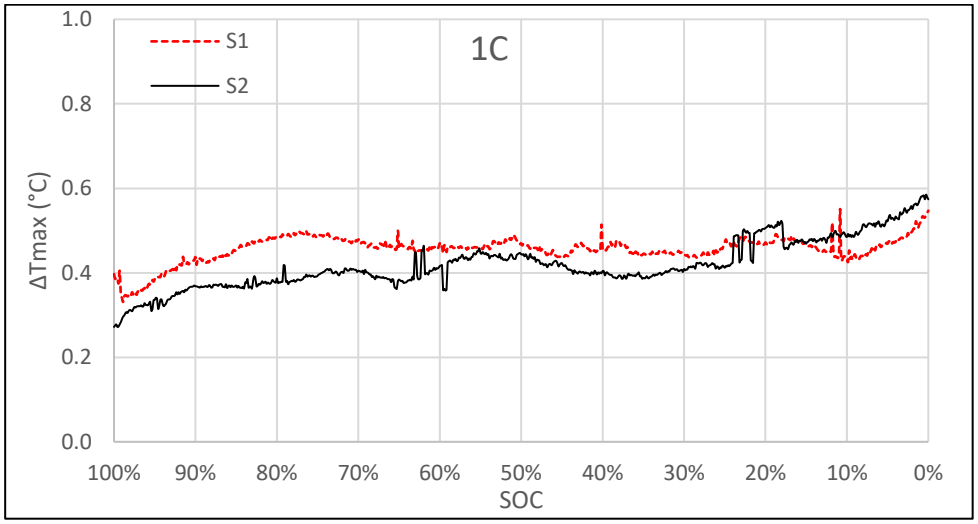

Figure 8. Maximum Surface Temperature Differences of S1 and S2 Systems at 20°C Ambient Temperature at 1C Discharge Rate

The total heat generated in the battery module at a discharge rate of 1C and an ambient temperature of 20°C was calculated in previous studies (Torun&Buyruk, 2024) and the maximum heat generation was found to be 2.30 W. Then, assuming that all the heat generated in the batteries is transmitted to the second block through the heat pipes, the difference in temperature values of the battery module to which the evaporator part of the heat pipe is connected and the second aluminium block to which the condenser part is connected is calculated with the help of equation (1) and given in Table 5.

Table 5. Maximum Heat and Temperature Difference Values at 1C Discharge Rate and 20°C Ambient Temperature in S1 and S2 Systems

	S1 System	S2 System
Q_{max} (W)	2,30	2,30
ΔT (K)	1,04	0,83

As a result, at 20°C ambient temperature and 1C discharge rate, the temperature difference between the first aluminium block and the second aluminium block decreased due to the use of a shorter heat pipe in the S2 system and the S2 system with a shorter heat pipe showed a better cooling performance by transmitting the heat generated in the batteries to the second block faster than the S1 system.

3.2. Performance of the Systems at 3C Discharge Rate

The maximum surface temperatures and maximum surface temperature differences of S1 and S2 modules obtained at 20°C ambient temperature and 3C discharge rate are given in Figure 9 and Figure 10.

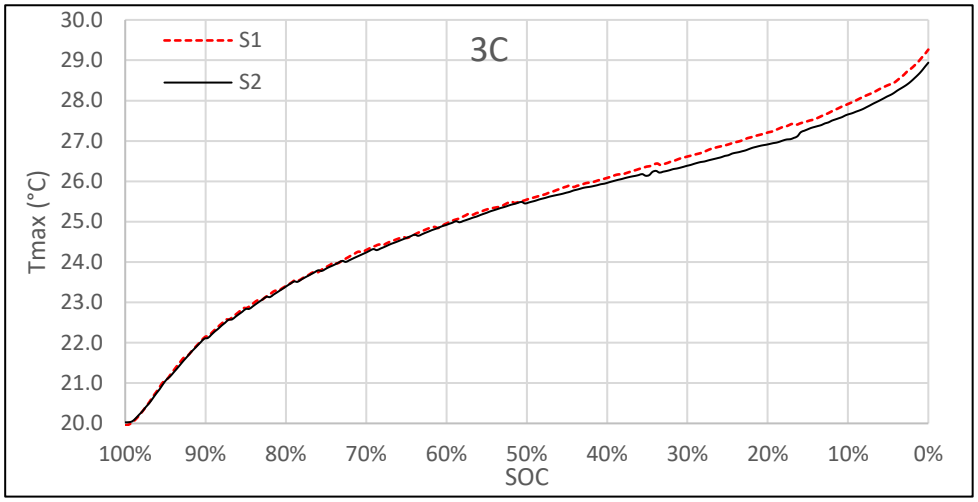

Figure 9. Maximum Surface Temperatures of S1 and S2 Systems at 20°C Ambient Temperature at 3C Discharge Rate

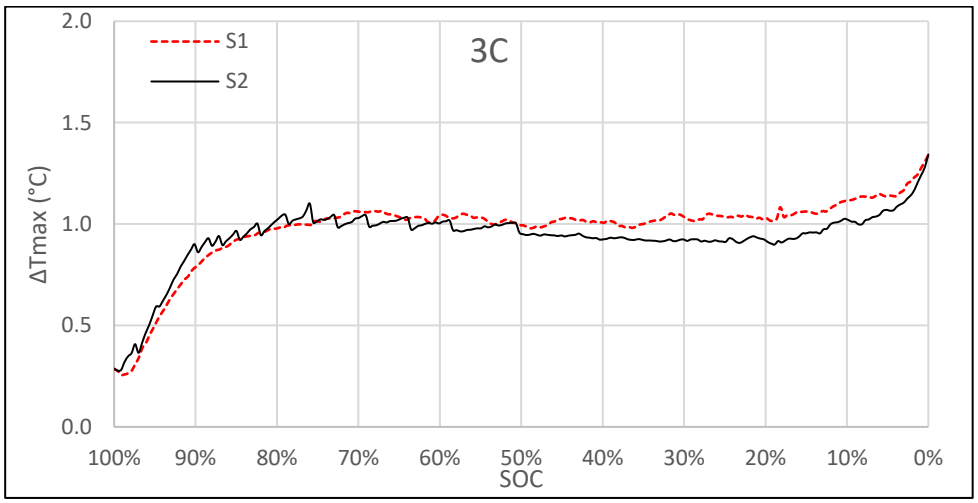

Figure 10. Maximum Surface Temperature Differences of S1 and S2 Systems at 20°C Ambient Temperature at 3C Discharge Rate

It was observed that the designed S2 module reduced the maximum surface temperature from 29.26°C to 28.94°C compared to the S1 module. It is also observed that the maximum battery surface temperature differences obtained in both systems are very close to each other and average 1.0°C. Therefore, S2 system exhibited a better cooling performance than S1 system at 3C discharge rate. In both cases, the maximum surface temperatures are below the permissible operating temperature of 40°C and the maximum surface temperature differences are below the permissible 5°C.

The total heat generated in the battery module at a discharge rate of 3C and ambient temperature of 20°C was calculated in previous studies (Torun and Buyruk, 2024) and assuming that all the heat generated in the batteries is transmitted to the second block through the heat pipes, the difference in temperature values of the battery module to which the evaporator part of the heat pipe is connected and the second aluminium block to which the condenser part is connected is calculated with the help of equation (1) and given in Table 6.

Table 6. Maximum Heat and Temperature Difference Values of S1 and S2 Systems at 3C Discharge Rate and 20°C Ambient Temperature

	S1 System	S2 System
Q_{max} (W)	11,86	11,86
ΔT (K)	5,36	4,29

As a result, at 20°C ambient temperature and 3C discharge rate, the temperature difference between the first aluminium block and the second aluminium block decreased due to the use of a shorter heat pipe in the S2 system and the S2 system with a shorter heat pipe showed a better cooling performance by transmitting the heat generated in the batteries to the second block faster than the S1 system.

3.3. Performance of the Systems at 5C Discharge Rate

Figure 11 and Figure 12 show the maximum surface temperatures and maximum surface temperature differences obtained from S1 and S2 modules at 20°C ambient temperature and 5C discharge rate.

It was observed that the designed S2 module reduced the maximum surface temperature from 34.12°C to 33.89°C compared to the S1 system. It is also observed that the maximum battery surface temperature differences obtained in both systems are very close to each other and average 1.5°C. Therefore, at 20°C ambient temperature and 5C discharge rate, the S2 system exhibited a better cooling performance than the S1 system, as in other discharge rates. In both cases, the maximum surface temperatures are below the permissible operating temperature of 40°C and the maximum surface temperature differences are below the permissible 5°C.

The total heat generated in the battery module at a discharge rate of 5C and an ambient temperature of 20°C was calculated in previous studies (Torun and Buyruk, 2024) and assuming that all the heat generated in the batteries is transmitted to the second block through the heat pipes, the difference in temperature values of the battery module to which the evaporator part of the heat pipe is connected and the second aluminium block to which the condenser part is connected is calculated with the help of equation (1) and given in Table 7.

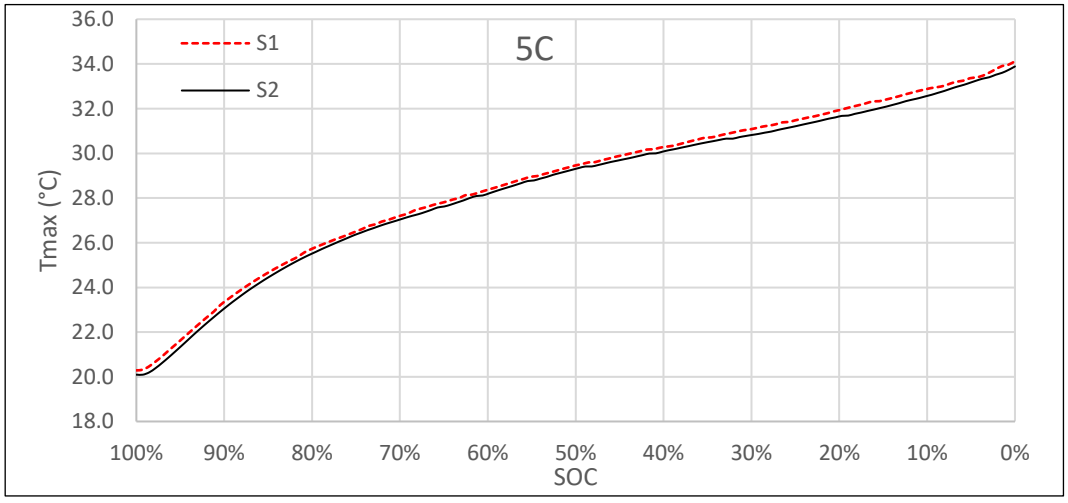

Figure 3. Maximum Surface Temperatures of S1 and S2 Systems at 20°C Ambient Temperature at 5C Discharge Rate

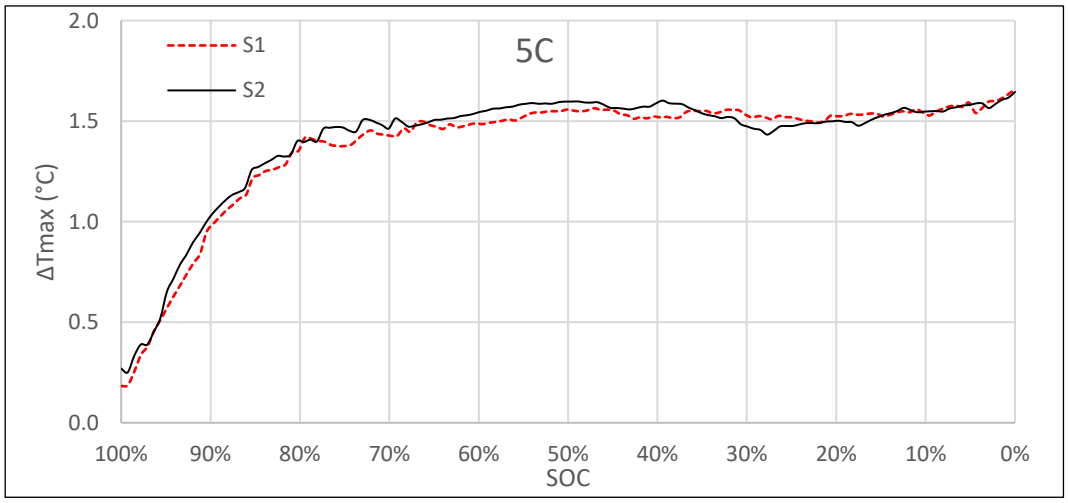

Figure 12. Maximum Surface Temperature Differences of S1 and S2 Systems at 20°C Ambient Temperature at 5C Discharge Rate

Table 7. Maximum Heat and Temperature Difference Values of S1 and S2 Systems at 5C Discharge Rate and 20°C Ambient Temperature

	S1 System	S2 System
Q_{max} (W)	32,98	32,98
ΔT (K)	14,91	11,93

As a result, at 20°C ambient temperature and 5C discharge rate, the temperature difference between the first aluminium block and the second aluminium block decreased due to the use of a shorter heat pipe in the S2 system and the S2 system with a shorter heat pipe showed a better cooling performance by transmitting the heat generated in the batteries to the second block faster than the S1 system.

4. Conclusion

Lithium-ion batteries release a large amount of heat energy when operating at high ambient temperatures and under severe operating conditions. The heat released also causes the temperature of the battery cells and the battery module to increase. In order to achieve maximum efficiency in lithium-ion batteries, the batteries should operate in the optimum temperature range of 15°C - 40°C and the maximum temperature difference between the battery cells forming the battery module should not exceed 5°C. In order to examine the effect of heat pipe length on battery cooling performance, two different systems consisting of heat pipes of different lengths, 15 and 17 cm, were designed, the designed system was discharged at a constant ambient temperature of 20°C and at different discharge rates of 1C, 3C and 5C, and the effect of heat pipe length on the cooling performance of the system was examined by comparing the maximum surface temperatures of the battery and the maximum surface temperature differences of the battery. As a result of the tests, it was determined that the calculated temperature difference between the condenser and evaporator sections of the heat pipe in the shorter heat pipe system (S2) is less than the temperature difference obtained in the longer pipe system (S1), so the short pipe S2 system conducts heat faster than the S1 system. It was observed that S2 system decreased the maximum battery surface temperature from 23.19°C to 22.93°C at 1C discharge rate, from 29.26°C to 28.94°C at 3C discharge rate and from 34.12°C to 33.89°C at 5C discharge rate compared to S1 system. In addition, it was calculated that the temperature difference between the evaporator and condenser parts of the heat pipe decreased from 1.04 °C in S1 system to 0.83 °C in S2 system at 1C discharge rate, from 5.36 °C in S1 system to 4.29 °C in S2 system at 3C discharge rate, and from 14.91 °C in S1 system to 11.93 °C in S2 system at 5C discharge rate, and it was determined that the S2 system with a shorter heat pipe cooled faster than the S1 system. This situation can be explained by the fact that the heat transfer rate passing through any medium is proportional to the inverse of the length of the medium it passes through. Therefore, the system with a shorter heat pipe transferred the heat to the external environment and the second aluminium block containing PCM more rapidly and a better cooling performance was obtained by reducing the maximum surface temperature of the battery more effectively. On the other hand, it was observed that the shorter the length of the adiabatic section and the closer the condenser and evaporator sections of the heat pipe are to each other, the better battery cooling performance can be obtained.

References

Behi, H., Karimi, D., Behi, M., Ghanbarpour, M., Jaguemont, J., Sokkeh, M. A., ... & Van Mierlo, J. (2020). A new concept of thermal management system in Li-ion battery using air cooling and heat pipe for electric vehicles. Applied Thermal Engineering, 174, 115280.

Belov, D., Yang, M. H. (2008). Failure mechanism of Li-ion battery at overcharge conditions. Journal of Solid State Electrochemistry, 12, 885-894.

Chen, K., Hou, J., Song, M., Wang, S., Wu, W., & Zhang, Y. (2021). Design of battery thermal management system based on phase change material and heat pipe. Applied Thermal Engineering, 188, 116665.

Etacheri, V., Marom, R., Elazari, R., Salitra, G. & Aurbach, D. (2011). Challenges in the development of advanced Li-ion batteries: a review. Energy & Environmental Science, 4(9), 3243-3262.

Faghri, A. (1995). Heat Pipe Science and Technology, Taylor & Francis. 32-35.

Ghanbarpourgeravi, M. (2017). Investigation of Thermal Performance of Cylindrical Heat pipes Operated with Nanofluids (Doctoral dissertation, KTH Royal Institute of Technology).

Greco, A., Jiang, X. & Cao, D. (2015). An investigation of lithium-ion battery thermal management using paraffin/porous-graphite-matrix composite, J. Power Sources, 278, 50–68.

Jouhara, H., Khordehgah, N., Serey, N., Almahmoud, S., Lester, S. P., Machen, D. & Wrobel, L. (2019). Applications and thermal management of rechargeable batteries for industrial applications. Energy, 170, 849-861.

Karimi, D., Hosen, M. S., Behi, H., Khaleghi, S., Akbarzadeh, M., Van Mierlo, J., & Berecibar, M. (2021). A hybrid thermal management system for high power lithium-ion capacitors combining heat pipe with phase change materials. Heliyon, 7(8).

Mahamud, R., Park, C. (2011). Reciprocating air flow for Li-ion battery thermal management to improve temperature uniformity. Journal of Power Sources, 196(13), 5685-5696.

Maleki, H., Howard, J. N. (2006). Effects of over discharge on performance and thermal stability of a Li-ion cell. Journal of power sources, 160(2), 1395-1402.

Park, C., Jaura, A. K. (2003). Dynamic thermal model of li-ion battery for predictive behaviour in hybrid and fuel cell vehicles (No. 2003-01-2286). SAE Technical Paper.

Pesaran, A. A. (2001). Battery thermal management in EV and HEVs: issues and solutions. Battery Man, 43(5), 34-49.

Pesaran, A. A. (2002). Battery thermal models for hybrid vehicle simulations. Journal of power sources, 110(2), 377-382.

Ramadass, P. H. B. W. R. P. B., Haran, B., White, R. & Popov, B. N. (2002). Capacity fade of Sony 18650 cells cycled at elevated temperatures: Part I. Cycling performance. Journal of power sources, 112(2), 606-613.

Rao, Z., Qian, Z., Kuang, Y. & Li, Y. (2017). Thermal performance of liquid cooling based thermal management system for cylindrical lithium-ion battery module with variable contact surface. Applied Thermal Engineering, 123, 1514-1522.

Song, L., Zhang, H. & Yang, C. (2019). Thermal analysis of conjugated cooling configurations using phase change material and liquid cooling techniques for a battery module. International Journal of Heat and Mass Transfer, 133, 827-841.

Tiari, S., Qiu, S. & Mahdavi, M. (2016). Discharging process of a finned heat pipe–assisted thermal energy storage system with high temperature phase change material. Energy Conversion and Management, 118, 426-437.

Torun, E. & Buyruk, E. (2024). Lityum İyon Pillerde Farklı Deşarj Hızlarında Oluşan Sıcaklık Profillerinin Deneysel ve Sayısal Olarak Karşılaştırılması. Osmaniye Korkut Ata Üniversitesi Fen Bilimleri Enstitüsü Dergisi, 7(2), 622-637.

Url-1 <https://www.nrel.gov/docs/fy13osti/58145.pdf>, alındığı tarih: 20.12.2022

Wu, W., Wang, S., Wu, W., Chen, K., Hong, S., & Lai, Y. (2019). A critical review of battery thermal performance and liquid based battery thermal management. Energy conversion and management, 182, 262-281.

Zhang, W., Qiu, J., Yin, X., & Wang, D. (2020). A novel heat pipe assisted separation type battery thermal management system based on phase change material. Applied Thermal Engineering, 165, 114571.